



# The *SCN8A* encephalopathy mutation p.Ile1327Val displays elevated sensitivity to the anticonvulsant phenytoin

\*†Bryan S. Barker, \*Matteo Ottolini, ‡Jacy L. Wagnon, ‡Rachel M. Hollander, ‡Miriam H. Meisler, and \*†Manoj K. Patel

*Epilepsia*, 57(9):1458–1466, 2016

doi: 10.1111/epi.13461

## SUMMARY

**Objective:** *SCN8A* encephalopathy (early infantile epileptic encephalopathy; EIEE13) is caused by gain-of-function mutations resulting in hyperactivity of the voltage-gated sodium channel  $Na_v1.6$ . The channel is concentrated at the axon initial segment (AIS) and is involved in establishing neuronal excitability. Clinical features of *SCN8A* encephalopathy include seizure onset between 0 and 18 months of age, intellectual disability, and developmental delay. Seizures are often refractory to treatment with standard antiepileptic drugs, and sudden unexpected death in epilepsy (SUDEP) has been reported in approximately 10% of patients. In a recent study, high doses of phenytoin were effective in four patients with *SCN8A* encephalopathy. In view of this observation, we have investigated the relationship between the functional effect of the *SCN8A* mutation p.Ile1327Val and its response to phenytoin.

**Methods:** The mutation was introduced into the *Scn8a* cDNA by site-directed mutagenesis. Channel activity was characterized in transfected ND7/23 cells. The effects of phenytoin (100  $\mu$ M) on mutant and wild-type (WT) channels were compared.

**Results:** Channel activation parameters were shifted in a hyperpolarizing direction in the mutant channel, whereas inactivation parameters were shifted in a depolarizing direction, increasing Na channel window current. Macroscopic current decay was slowed in I1327V channels, indicating an impairment in the transition from open state to inactivated state. Channel deactivation was also delayed, allowing more channels to remain in the open state. Phenytoin (100  $\mu$ M) resulted in hyperpolarized activation and inactivation curves as well as greater tonic block and use-dependent block of I1327V mutant channels relative to WT.

**Significance:** *SCN8A* – I1327V is a gain-of-function mutation with altered features that are predicted to increase neuronal excitability and seizure susceptibility. Phenytoin is an effective inhibitor of the mutant channel and may be of use in treating patients with gain-of-function mutations of *SCN8A*.

**KEY WORDS:** *SCN8A*, Anticonvulsant drugs, Sodium channels, Epileptic encephalopathy, Phenytoin.



Bryan Barker is a neuroscience doctoral candidate at the University of Virginia.

Accepted June 10, 2016; Early View publication July 4, 2016.

\*Department of Anesthesiology, University of Virginia Health System, Charlottesville, Virginia, U.S.A.; †Neuroscience Graduate Program, University of Virginia Health System, Charlottesville, Virginia, U.S.A.; and ‡Department of Human Genetics, University of Michigan, Ann Arbor, Michigan, U.S.A.

Address correspondence to Manoj K. Patel, Department of Anesthesiology, University of Virginia Health System, Charlottesville, VA 22908-0710, U.S.A. E-mail: mkp5u@virginia.edu

Wiley Periodicals, Inc.

© 2016 International League Against Epilepsy

Sodium (Na) channels play a critical role in controlling neuronal excitability because they are directly involved in action potential generation and conduction, and also play a role in the transition between single spiking and bursting in some neurons.<sup>1</sup> Proexcitatory alterations in Na channel function have been reported in patients with epilepsy,<sup>2,3</sup> and in animal models of epilepsy.<sup>4,5</sup> The Na channel isoform  $Na_v1.6$  is encoded by the *SCN8A* gene and is highly localized along the axonal initial segment (AIS),<sup>6</sup> the site of

## KEY POINTS

- The *SCN8A* mutation I1327V was previously identified in two patients with early infantile epileptic encephalopathy (EIEE13)
- Electrophysiologic analysis of I1327V demonstrated altered activation and inactivation parameters that are pro-excitatory
- Deactivation and transition from open state to inactivated state were impaired
- The effect of the anticonvulsant drug phenytoin on tonic inhibition and use-dependent block was greater on mutant than on wild-type channels
- Phenytoin may be effective in suppressing seizures in some *SCN8A* gain-of-function mutations

action potential generation, and at the nodes of Ranvier.<sup>7</sup> In some acquired epilepsy, Na<sub>v</sub>1.6 expression is increased,<sup>4,5</sup> and reducing Na<sub>v</sub>1.6 has been shown to impair the initiation and development of kindled seizures.<sup>4</sup>

De novo missense mutations of *SCN8A* are associated with early infantile epileptic encephalopathy (EIEE).<sup>26</sup> Since the discovery of the first mutation,<sup>8</sup> >100 additional mutations have been identified and collectively defined as EIEE13.<sup>3</sup> Most patients with EIEE13 have seizure onset between birth and 12 months of age, with a median age of onset of 4 months. After the onset of seizures, there is significant developmental regression that results in mild to severe intellectual disability. Sudden unexpected death in epilepsy (SUDEP) has been reported in approximately 10% of patients.

Electrophysiology studies on a limited number of mutations demonstrate that many have a gain-of-function characteristic.<sup>8,10,15</sup> Of interest, the mechanism by which this proexcitatory endpoint is achieved differs among the mutations. In some, there is an increase in persistent Na current and proexcitatory shifts in channel inactivation parameters, whereas in others there is a leftward shift in the voltage dependence of activation. A knock-in mouse model carrying the *SCN8A* mutation p.Asn1768Asp possesses many of the pathologic phenotypes seen in human patients, including seizures and sudden death.<sup>11</sup>

Because the seizures in many EIEE13 patients are associated with a gain-of-function in Na channel activity, a rational approach to therapy would be to use anticonvulsants with Na channel blocking characteristics. However, the seizures in EIEE13 patients are difficult to control even with Na channel blockers, and many patients remain refractory. A recent study of four children with EIEE13 demonstrated good seizure control with high doses of phenytoin.<sup>12</sup> One of these patient mutations included in the study has been examined functionally and shown to result in a

hyperpolarizing shift in voltage dependence of activation.<sup>9</sup> In the current study, we determined the biophysical properties of another *SCN8A* mutation, p.Ile1327Val, located within the highly conserved region of transmembrane segment 5 adjacent to the cytosolic interface of the S4–S5 linker of domain III.<sup>13,19</sup> Our data show that I1327V is a gain-of-function mutation that is predicted to lead to increased neuronal activity and the generation of seizures. We demonstrate that phenytoin (100 μM) results in greater tonic block and use-dependent block of I1327V channels compared with WT channels. The preferential effect of phenytoin on the mutant channel may increase the effectiveness of phenytoin in treating refractory seizures associated with EIEE13.

## METHODS

### Site-directed mutagenesis of the Na<sub>v</sub>1.6 cDNA

The amino acid substitution I1327V was introduced into the tetrodotoxin (TTX)-resistant derivative of the full-length rNa<sub>v</sub>1.6 cDNA clone (NM\_014191.3, NP\_055006.1),<sup>14</sup> as described previously.<sup>8,9,15</sup> Site-directed mutagenesis was carried out with the QuikChange II XL kit (Agilent Technologies). The entire 6-kb open reading frame was sequenced to confirm the absence of other mutations.

### Cell culture

Dorsal root ganglion (DRG)-neuron derived ND7/23 cells (Sigma Aldrich) were grown in a humidified atmosphere of 5% CO<sub>2</sub> and 95% air at 37°C in Dulbecco's Modified Eagle Medium (DMEM 1×) supplemented with 10% Fetal Bovine Serum (FBS), Non-Essential Amino Acid (NEAA), and sodium pyruvate. Cells were plated onto petri dishes 48 h prior to transfection and transfected for 5 h in nonsupplemented DMEM using lipofectamine 3000 according to manufacturer instructions (Life Technologies) with 5 μg of Na<sub>v</sub>1.6 alpha subunit cDNA and 0.5 μg of the fluorescent m-Venus bioreporter. Electrophysiologic recordings of fluorescent cells were made 48 h after transfection.

### Electrophysiology

Recordings were carried out in the presence of 500 nM TTX to block endogenous sodium currents in the neuron-derived ND7/23 cells. Currents were recorded using the whole-cell configuration of the patch-clamp recording technique as described previously.<sup>15</sup> Currents were amplified and low-pass filtered (2 kHz) and sampled at 33 kHz. The intracellular recording solution contained (in mM): 140 CsF, 2 MgCl<sub>2</sub>, 1 EGTA, 10 HEPES, 4 Na<sub>2</sub>ATP, 0.3 NaGTP (pH adjusted to 7.2 with CsOH, osmolarity adjusted to 300 mOsm with sucrose). Cultured ND7/23 cells were bathed in solution containing (in mM): 130 NaCl, 3 KCl, 1 CaCl<sub>2</sub>, 5 MgCl<sub>2</sub>, 0.1 CdCl<sub>2</sub>, 10 HEPES, 30 TEA (pH adjusted to 7.4 with NaOH, osmolarity adjusted to 310 mOsm with sucrose). Experiments were performed at room temperature (20–22°C). After establishing the whole

cell configuration, a minimum series resistance compensation of 75% was applied. Capacitive and leak currents were subtracted using the P/4 protocol for all experiments, except steady-state inactivation protocols. The current–voltage relationship was determined using a 100 msec voltage pulse from  $-80$  to  $+70$  mV in steps of 5 mV from a holding potential of  $-120$  mV at 2 s intervals. Conductance as a function of voltage was derived from the current–voltage relationship and fitted by a Boltzmann function as described.<sup>5</sup> Decays of macroscopic currents were fitted to a single exponential function, and time constants were determined. For steady-state inactivation, neurons were held at  $-120$  mV and test potentials from  $-115$  to  $-10$  mV for 500 msec at 5 mV increments were applied. The second pulse to  $-10$  mV for 40 msec was used to assess channel availability. Correction for passive and leak currents was achieved by subtracting the last sweep with the greatest depolarizing potential ( $-10$  mV), since this sweep displays no sodium channel current. Currents during the second pulse were normalized for each cell with the largest current as 1.0 and fit to the Boltzmann function. Deactivation was estimated from current decay, using a 0.5 msec short depolarizing pulse to  $-10$  mV followed by a 50 msec repolarizing pulse to potentials ranging from  $-40$  to  $-120$  mV at 5 mV increments. Deactivation kinetics were determined by fitting decaying currents with a single exponential function. For recovery from inactivation, cells were held at  $-120$  mV and depolarized to a test potential of 0 mV for 1 s to inactivate Na channels. Recovery was determined at times between 1 msec and 60 s at a test potential of  $-90$  mV. A 40 msec pulse to  $-10$  mV was subsequently applied to assess the extent of channel recovery. For each cell, current amplitudes during the test pulse were normalized so that the largest current during the conditioning potential was 1.0. Data were then fit to a double exponential function as described previously.<sup>5</sup>

For experiments involving the testing of phenytoin, electrophysiologic protocols under control, drug-free conditions were obtained before bath application of phenytoin ( $100 \mu\text{M}$ ; 10 min).

### Data analysis

Data represent means  $\pm$  standard error of the mean (SEM). Statistical significance was determined using a Student's *t*-test or a standard one way analysis of variance (ANOVA) followed by Tukey's or Dunn's post hoc test for parametric data or the rank sum test for nonparametric data (GraphPad Prism 6).

## RESULTS

### Electrophysiologic characterization of I1327V

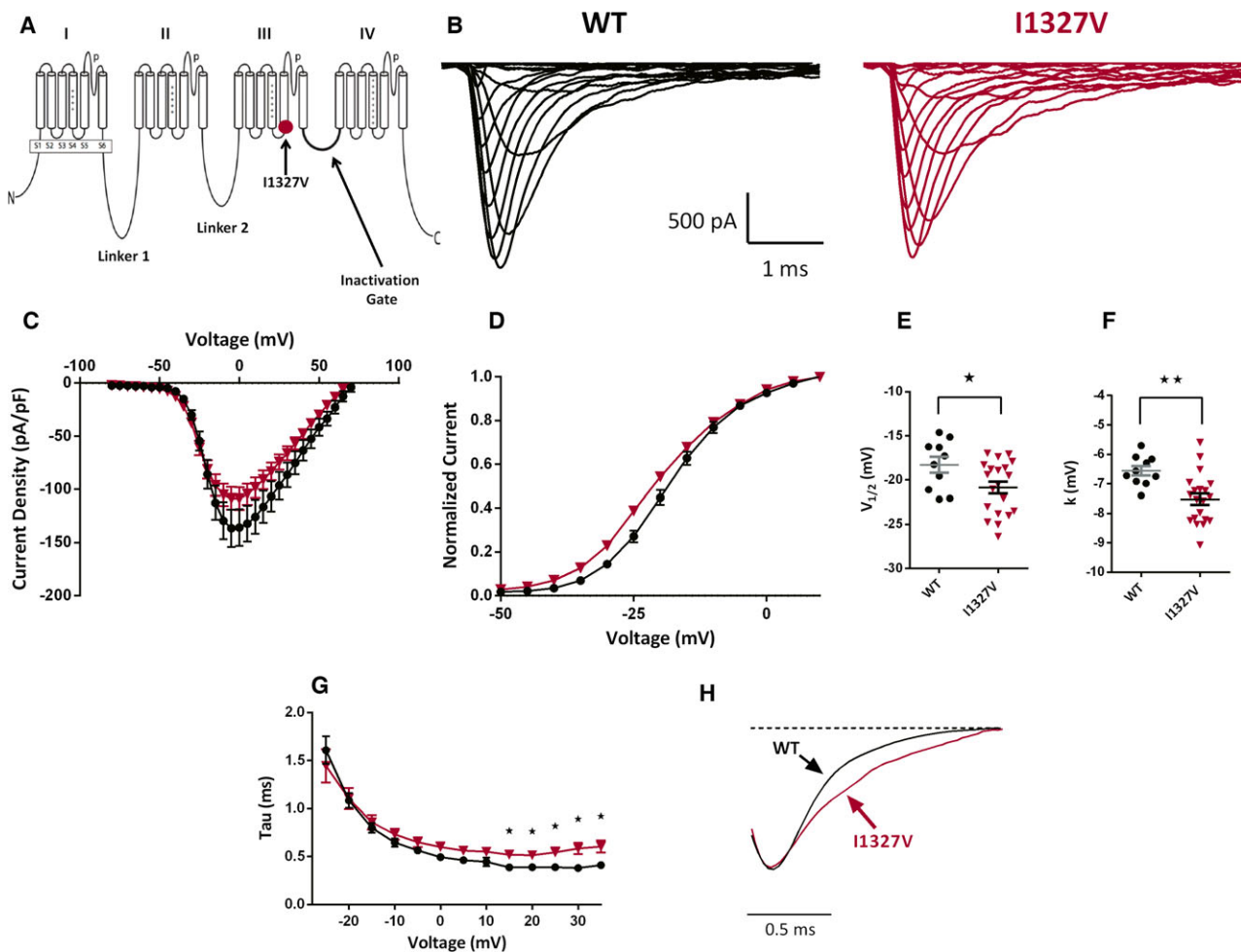
Isoleucine residue 1327 is located in the highly conserved region of transmembrane segment 5 of domain III (D3S5) adjacent to the cytosolic S4–S5 linker of  $\text{Na}_v1.6$  (Fig. 1A).

Representative currents from ND7/23 cells transfected with WT and I1327V  $\text{Na}_v1.6$  are shown in Figure 1B. Peak current density for I1327V was not elevated compared to WT (Fig. 1C). Analysis of steady-state kinetics demonstrates a small but significant hyperpolarizing shift in the half maximal voltage dependence of activation for I1327V ( $V_{1/2}$ ) of  $-2.5$  mV ( $p < 0.05$ ; Fig. 1D,E). Slope factor ( $k$ ) was also significantly decreased ( $p < 0.005$ ; Fig. 1F, Table 1). To determine the kinetics of open state inactivation, macroscopic current decay was fit to single exponential functions and the fast time constant ( $T$ ) was plotted as a function of voltage. Transition from open state to the inactivated state was significantly delayed in I1327V channels at depolarizing voltages ranging between  $+15$  and  $+35$  mV (Fig. 1G), consistent with the prediction of disrupted inactivation. The slowing of fast inactivation is evident when the peaks of the current traces at  $+35$  mV are aligned so that inactivation kinetics can be compared directly (Fig. 1H). When examined at a time point of 100 msec after the voltage stimulus, decay of macroscopic current was complete for both I1327V and WT, indicating the absence of increased persistent current in the mutant channel (data not shown).

We next determined the effects of I1327V on the kinetics of channel deactivation. Compared to WT channels, I1327V significantly increased the time constant ( $T$ ) of deactivation over the range of voltages between  $-55$  and  $-40$  mV (Fig. 2A), indicating a slower transition from the open state back to the closed state. Disruption in normal inactivation processes have been described for several *SCN8A* mutations.<sup>15</sup> In I1327V channels, a significant depolarizing shift in the  $V_{1/2}$  of steady-state inactivation was recorded ( $5.7$  mV;  $p < 0.005$ ; Fig. 2B,C) with no change in slope values (Fig. 2D). Window currents can be determined by taking the area under the overlapping normalized activation and inactivation curves (Fig. 2E).<sup>16</sup> We determined the window current for I1327V and WT channels and found an increase in the window current for the mutant channel (Fig. 2F). Finally, we examined recovery from inactivation using a recovery voltage of  $-90$  mV and found no significant difference between WT and I1327V transfected cells (Fig. 2G; Table 1).

### Inhibition of I1327V by phenytoin

The antiepileptic drug (AED) phenytoin (Dilantin<sup>®</sup>) is clinically used to treat epileptic seizures. The mechanism is thought to involve the inhibition of Na channels.<sup>17</sup> Phenytoin binds preferentially to the inactivated form of  $\text{Na}_v1.6$ , and the drug can block high frequency firing of action potentials, thereby trapping channels in the inactivated state.<sup>17</sup> Because I1327V displayed disrupted inactivation parameters, we sought to determine if phenytoin would inhibit currents evoked from a holding potential of  $-60$  mV, a potential when many of the channels can cycle between the closed, open, and inactivated states. At a concentration of  $100 \mu\text{M}$ , tonic block by phenytoin was significantly greater

**Figure 1.**

I1327V modulates steady-state activation. **(A)** Four-domain structure of the voltage-gated Na channel  $\alpha$  subunit shows that I1327V is located at the cytosolic interface of the S4–S5 linker and transmembrane segment 5 of domain III. **(B)** Representative traces of families of Na currents recorded from ND7/23 cells transfected with the indicated  $\text{Na}_v1.6$  cDNAs. **(C)** Averaged current-voltage ( $I$ - $V$ ) relationship for cells expressing WT and I1327V. Peak currents were normalized to cell capacitance. **(D)** Voltage dependence of channel activation. Smooth lines correspond to the least-squares fit when average data were fit to a single Boltzmann equation. **(E)** Scatter plot of voltage at half-maximal activation ( $V_{1/2}$ ) for cells expressing WT and I1327V. **(F)** Scatter plot of the slope factor of activation ( $k$ ). **(G)** Average fast time constants obtained from single exponential fits to macroscopic current decays as a function of voltage. **(H)** Representative traces of normalized currents evoked by a +35 mV stimulus from a holding potential of -120 mV illustrate delays in macroscopic current decay between WT (black) and I1327V (red). Data are means  $\pm$  SEM. Statistical significance: \* $p < 0.05$ ; \*\* $p < 0.005$ . Black circles, WT; red triangles, I1327V.

Epilepsia © ILAE

**Table 1. Biophysical properties of I1327V and WT channels**

|        | Activation        |                     |     | Inactivation         |               |     | Recovery       |                 |                |     |
|--------|-------------------|---------------------|-----|----------------------|---------------|-----|----------------|-----------------|----------------|-----|
|        | $V_{1/2}$         | $k$                 | $n$ | $V_{1/2}$            | $k$           | $n$ | $\tau_1$       | $\tau_2$        | %Fast          | $n$ |
| WT     | $-18.3 \pm 0.9$   | $-6.6 \pm 0.2$      | 10  | $-69.4 \pm 1.8$      | $7.3 \pm 0.2$ | 19  | $390 \pm 85.8$ | $6,614 \pm 799$ | $47.6 \pm 0.1$ | 19  |
| I1327V | $-20.8 \pm 0.7^*$ | $-7.5 \pm 0.2^{**}$ | 20  | $-63.7 \pm 0.6^{**}$ | $7.3 \pm 0.2$ | 33  | $577 \pm 50.8$ | $6,020 \pm 380$ | $45.2 \pm 0.1$ | 33  |

$n$ , number of cells;  $V_{1/2}$ , voltage of half-maximal activation or inactivation;  $k$ , slope factor.

Values represent means  $\pm$  SEM.

Significance was determined by unpaired Student's  $t$ -test \* $p < 0.05$ , \*\* $p < 0.005$ .



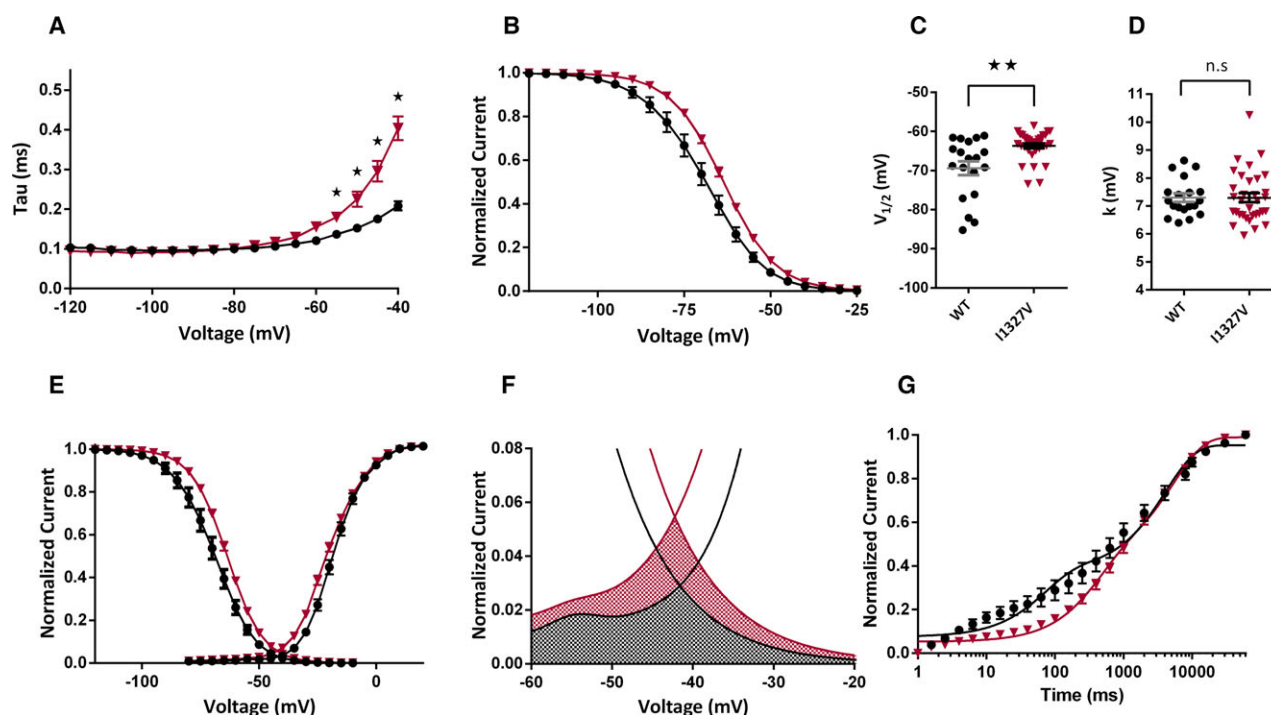


**Figure 2.**

I1327V disrupts channel inactivation properties. **(A)** Average fast time constant obtained from single exponential fits to deactivation of WT and I1327V channels. **(B)** Voltage dependence of steady-state inactivation. Smooth lines correspond to the least-squares fit when average data were fit to a single Boltzmann equation. **(C)** Scatter plot of the voltage at half-maximal inactivation ( $V_{1/2}$ ) for cells expressing WT and I1327V. **(D)** Scatter plot of the slope factor ( $k$ ) of inactivation. **(E)** The window current is obtained by overlapping the normalized activation and inactivation curves from WT and I1327V cells. **(F)** Enhanced view of overlapping activation and inactivation curves shows an increase in I1327V window current (red shaded area) compared to WT (gray shaded area). **(G)** Recovery from inactivation at a post train level of  $-90$  mV. Data are means  $\pm$  SEM. Statistical significance: \* $p < 0.05$ ; \*\* $p < 0.005$ . Black circles, WT; red triangles, I1327V.

*Epilepsia* © ILAE

for I1327V ( $53 \pm 2.0\%$ ;  $n = 10$ ) than WT currents ( $43 \pm 2.0\%$ ;  $n = 8$ ;  $p < 0.05$ ; Fig. 3A,B). In addition to voltage-dependent block, AEDs also exhibit use-dependent block as an important mechanism of action, permitting enhanced block of high-frequency neuronal firing associated with epileptic seizures.<sup>18</sup> In a manner similar to that of tonic block, phenytoin ( $100 \mu\text{M}$ ) produced a greater use-dependent block of I1327V channels compared to WT (Fig. 3C). In the absence of phenytoin, there was very little block of control ( $6.0 \pm 1.0\%$ ;  $n = 23$ ) and I1327V ( $7.0 \pm 1.0\%$ ;  $n = 29$ ) channel currents during the use-dependent protocol. In the presence of phenytoin, WT channels were blocked by  $11 \pm 2.0\%$  ( $n = 12$ ) at pulse 60. In contrast, phenytoin caused greater use-dependent block of I1327V channels, blocking the current by  $21 \pm 4.0\%$  ( $n = 9$ ;  $p < 0.05$ ).

Phenytoin ( $100 \mu\text{M}$ ) also caused a hyperpolarizing shift in the voltage dependence of activation for both WT channel ( $V_{1/2}$  by  $-7.6$  mV;  $p < 0.05$ ; Fig. 3D,E) and I1327V channels ( $V_{1/2}$  by  $-16.9$  mV;  $p < 0.05$ ; Fig. 3F,G). Phenytoin had no effect on the slope ( $k$ ) in WT or I1327V channels (Table 2). Inactivation parameters were shifted

significantly in a hyperpolarized direction by phenytoin ( $100 \mu\text{M}$ ) for both WT ( $V_{1/2}$  by  $-15.4$  mV;  $p < 0.05$ ; Fig. 4A–C) and I1327V ( $V_{1/2}$  by  $-13.0$  mV;  $p < 0.005$ ; Fig. 4D–F). Slope factors ( $k$ ) remained unchanged for both WT and I1327V (Table 2). Phenytoin did not significantly alter either the fast or slow time constants of recovery from inactivation at  $-90$  mV in either I1327V- or WT-transfected cells (Table 2). Phenytoin did, however, significantly decrease the amplitude of the Na current recorded after a recovery interval of 60 s in WT ( $47.3 \pm 3.4\%$  Fig. 4G) and I1327V ( $33.6 \pm 11.3\%$  Fig. 4H).

## DISCUSSION

The de novo mutation I1327V was identified in two unrelated patients with early onset encephalopathy.<sup>13,19</sup> Residue Ile1327 is located within the highly conserved region of transmembrane segment D3S5 adjacent to the cytosolic interface with the S4–S5 linker. Mutation studies indicate that residues located along the S4–S5 linker of domain III are critical to fast inactivation, since they provide an interaction site for the fast inactivation gate.<sup>20</sup> Because isoleucine

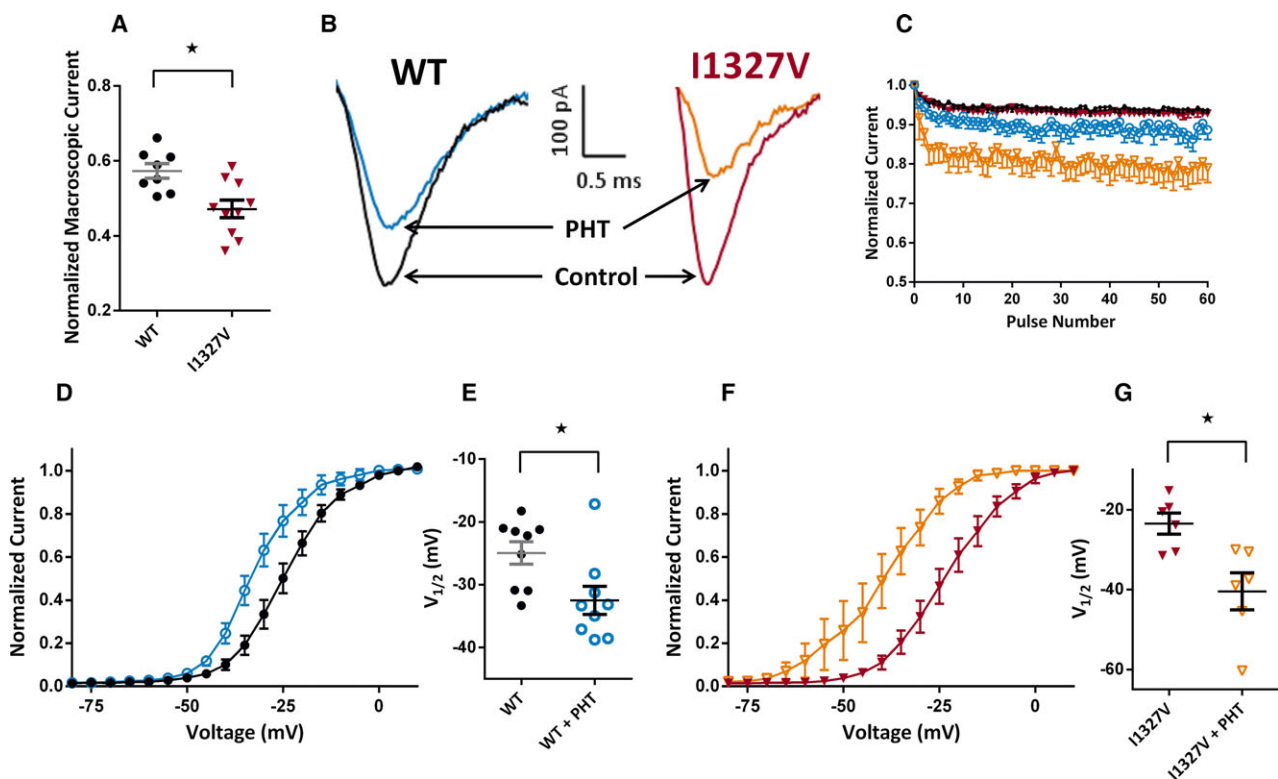


**Figure 3.**

Phenytoin (PHT) inhibits Na channel currents evoked from WT and I1327V and modulates steady-state activation parameters. **(A)** Scatter plot showing normalized macroscopic current amplitude remaining following tonic block by phenytoin ( $100\ \mu\text{M}$ ). Currents were elicited by a depolarizing step to  $0\ \text{mV}$  for  $12\ \text{msec}$  from a holding potential of  $-60\ \text{mV}$ . **(B)** Representative traces show greater tonic inhibition of I1327V currents over WT currents by phenytoin ( $100\ \mu\text{M}$ ). **(C)** Use-dependent block by phenytoin ( $100\ \mu\text{M}$ ). Cells were held at  $-120\ \text{mV}$  and a voltage step to  $+20\ \text{mV}$  was applied for  $20\ \text{msec}$  at a frequency of  $10\ \text{Hz}$ . **(D)** Shift in the voltage dependence of WT channel activation following treatment with phenytoin ( $100\ \mu\text{M}$ ). Smooth lines correspond to the least squares fit when average data were fit to a single Boltzmann equation. **(E)** Scatter plot of voltage at half-maximal activation ( $V_{1/2}$ ). **(F)** Shift in the voltage dependence of I1327V channel activation following treatment with phenytoin ( $100\ \mu\text{M}$ ). Smooth lines correspond to the least squares fit when average data were fit to a single Boltzmann equation. **(G)** Scatter plot of voltage at half-maximal activation ( $V_{1/2}$ ). Data are means  $\pm$  SEM. Statistical significance: \* $p < 0.05$ . Black filled circles, WT; blue open circles, WT + phenytoin, red filled triangles, I1327V; orange open triangles, I1327V + phenytoin.

*Epilepsia* © ILAE

**Table 2. Phenytoin ( $100\ \mu\text{M}$ ) modulates the biophysical properties of I1327V and WT channels**

|              | Activation        |                |   | Inactivation         |               |   | Recovery        |                    |                |   |
|--------------|-------------------|----------------|---|----------------------|---------------|---|-----------------|--------------------|----------------|---|
|              | $V_{1/2}$         | k              | n | $V_{1/2}$            | k             | n | $\tau_1$        | $\tau_2$           | %Fast          | n |
| WT           | $-24.9 \pm 1.8$   | $-6.3 \pm 0.2$ | 9 | $-66.2 \pm 4.1$      | $7.2 \pm 0.3$ | 6 | $181 \pm 95$    | $4,405 \pm 1,196$  | $56.4 \pm 0.1$ | 7 |
| WT + PHT     | $-32.5 \pm 2.2^*$ | $-5.8 \pm 0.5$ | 9 | $-81.6 \pm 5.1^*$    | $7.9 \pm 0.4$ | 6 | $145 \pm 57$    | $4,942 \pm 1,757$  | $51.6 \pm 0.1$ | 7 |
| I1327V       | $-23.5 \pm 2.6$   | $-7.3 \pm 0.2$ | 6 | $-65.3 \pm 2.0$      | $7.4 \pm 0.4$ | 9 | $423 \pm 205$   | $8,668 \pm 122$    | $44.4 \pm 0.1$ | 5 |
| I1327V + PHT | $-40.4 \pm 4.6^*$ | $-6.2 \pm 0.5$ | 6 | $-78.3 \pm 2.7^{**}$ | $8.6 \pm 0.4$ | 9 | $1,044 \pm 647$ | $11,858 \pm 2,902$ | $45.4 \pm 0.1$ | 5 |

n, number of cells;  $V_{1/2}$ , voltage of half-maximal activation or inactivation; k, slope factor.  
 Values represent means  $\pm$  SEM.  
 Significance was determined by paired Student's *t*-test \* $p < 0.05$  to pre-phenytoin condition, \*\* $p < 0.005$  to pre-phenytoin condition.

and valine are relatively similar in structure and both are nonpolar, hydrophobic amino acids, the mechanisms behind disrupted inactivation are not obvious. We hypothesize that substituting the bulky isoleucine side chain with methyl and ethyl groups, for the smaller valine side chain, composed

only of methyl groups, may disrupt the hydrogen bonds that form between the inactivation gate and the S4–S5 linker of domain III, disrupting the normal inactivation process.

Consistent with the gain-of-function mechanism, I1327V resulted in a hyperpolarizing shift in activation parameters,

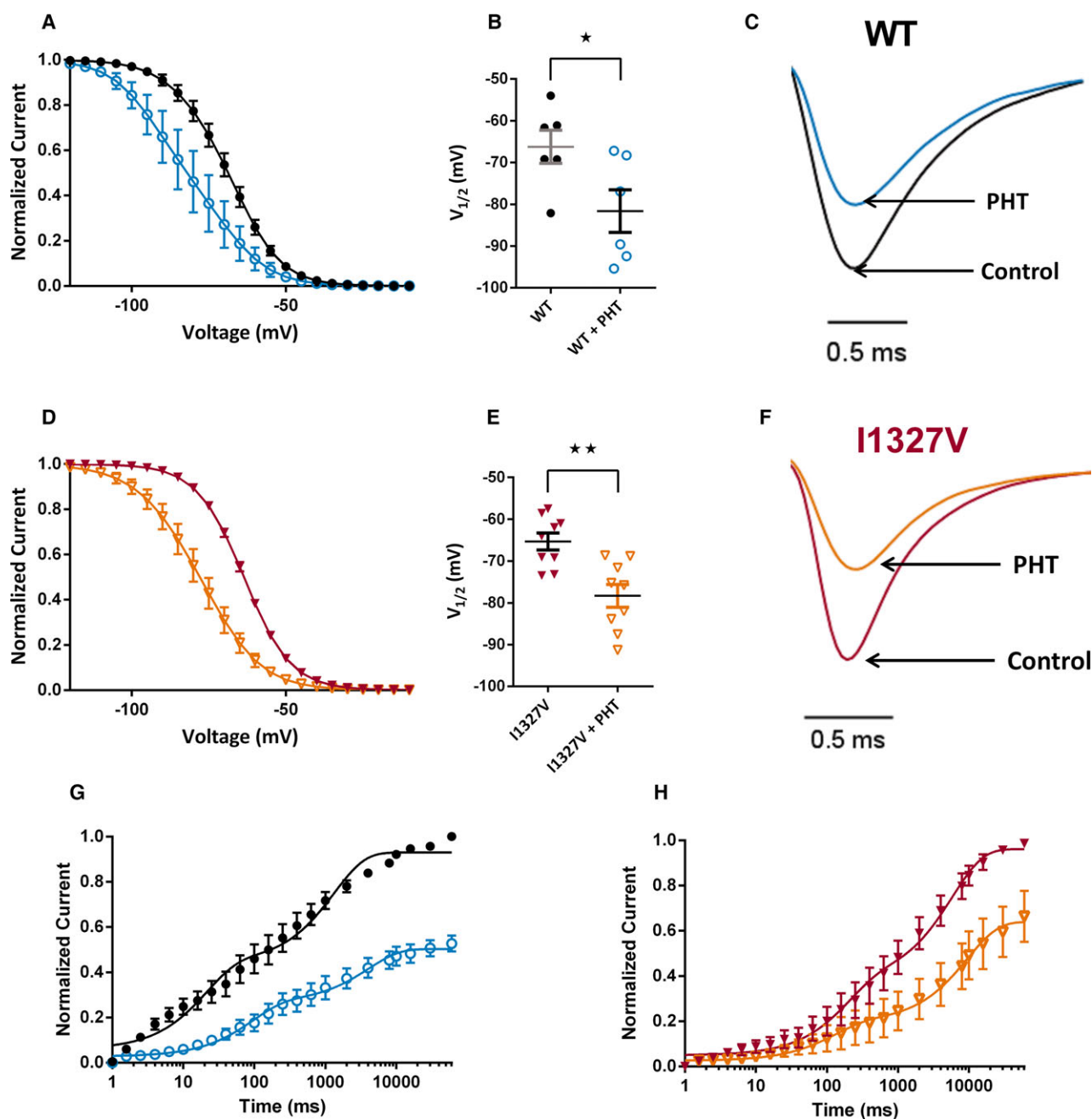


**Figure 4.**

Phenytoin (PHT) modulates steady state inactivation properties in cells expressing WT and I1327V channels. **(A)** Shift in the voltage dependence of WT channel inactivation following treatment with phenytoin (100  $\mu\text{M}$ ). Smooth lines correspond to the least-squares fit when average data were fit to a single Boltzmann equation. **(B)** Scatter plot of voltage at half-maximal inactivation ( $V_{1/2}$ ). **(C)** Representative WT traces elicited following a pre-pulse to  $-75$  mV demonstrating the shift in inactivation following application of phenytoin (100  $\mu\text{M}$ ). Traces were normalized to the pre-phenytoin peak current. **(D)** Shift in the voltage dependence of I1327V channel inactivation following treatment with phenytoin (100  $\mu\text{M}$ ). Smooth lines correspond to the least-squares fit when average data were fit to a single Boltzmann equation. **(E)** Scatter plot of voltage at half-maximal inactivation ( $V_{1/2}$ ). **(F)** Representative I1327V traces following a pre-pulse to  $-75$  mV demonstrating the shift in inactivation following the application of phenytoin (100  $\mu\text{M}$ ). Recovery from inactivation before and after the application of phenytoin (100  $\mu\text{M}$ ) in WT **(G)** and I1327V **(H)** cells. Data are means  $\pm$  SEM. Statistical significance \* $p < 0.05$ ; \*\* $p < 0.005$ . Black-filled circles, WT; blue open circles, WT + phenytoin; red-filled triangles, I1327V; orange open triangles, I1327V + phenytoin.

Epilepsia © ILAE

enabling mutant channels to open at voltages more negative than WT channels. This shift, coupled with a depolarizing shift in the voltage dependence of inactivation, would extend the voltage range where channels would be available for activation and have a finite probability of opening. This range of voltages is commonly referred to as the window current, and an enhancement in this current would reduce action potential thresholds, thereby facilitating action potential firing and potentially initiating seizure generation and spread. Increases in window currents have been associated with increased persistent sodium current activity and epileptogenesis in animal models.<sup>21,22</sup> A delay in the decay of the macroscopic current at depolarized voltages further supports the view that a valine for isoleucine substitution at position 1327 results in a major disruption of the normal inactivation process in the mutant channel, specifically delaying entry into the inactivated state. A slowing in channel deactivation would increase the availability of Na channels by delaying the transition of open channels back into the closed state during short depolarizations, further increasing the probability that channels remain in the open state configuration for longer periods.

There is considerable heterogeneity among the 10 *SCN8A* mutations that have now been characterized through electrophysiology studies. One common pathogenic mechanism is a disruption in the inactivation process. In some cases, including the current mutation I1327V, this is due to a depolarizing shift in the inactivation curve that delays channel inactivation,<sup>10</sup> whereas other mutations have normal voltage dependence of inactivation with an increase in persistent Na channel current after prolonged depolarization.<sup>8</sup> Many of these mutations are located at sites involved in channel inactivation, including domain III, domain IV, and the C-terminus.<sup>3</sup> In contrast, two mutations located within transmembrane segments of domain II have normal inactivation parameters, but establish a gain-of-function phenotype via hyperpolarizing activation curves, thereby increasing channel availability at more negative membrane potentials and consequently increasing window currents.<sup>9,10</sup>

AEDs that inhibit Na channels as a mechanism of action have been used in treating seizures in patients with EIEE13. However, it is unclear which AEDs should be considered first for these patients. Furthermore, mechanistic studies demonstrating the response of mutant channel currents to AEDs are lacking. In a recent study of four patients with seizures that were refractory to many AEDs, good seizure control was obtained with high-dose phenytoin.<sup>12</sup> Withdrawal of phenytoin resulted in seizure reoccurrence in all four patients. This work suggests that phenytoin may be more effective for *SCN8A* encephalopathy than other clinically available AEDs. The mode of action of phenytoin includes inhibition of Na channels, but it also effects calcium channels.<sup>17,23</sup> Phenytoin has little effect on Na channels in their resting or closed state, but at more depolarized potentials,

such as those observed during high frequency firing, the block by phenytoin is pronounced.<sup>17,24</sup> This greater affinity for the inactivated state of the channel over the closed state of the channel is an important characteristic of many AEDs.<sup>25</sup> When tested on the mutation I1327V, tonic block and use-dependent block by phenytoin was more pronounced for the mutant channel than for the WT channels. A likely explanation is that phenytoin binds slowly to open and inactivated channels.<sup>17</sup> The mutant channel displayed impaired deactivation kinetics and slowed transition from the open state to the inactivated state at depolarized voltages, allowing channels to remain longer in nonclosed conformation. Increased proportion of channels in open and inactivated states would increase the time available for phenytoin to bind tightly and trap the mutant channels in a nonconducting conformation, thereby preventing them from contributing to action potential initiation. This feature is referred to as the modulated receptor hypothesis.<sup>27</sup> Phenytoin also reversed the depolarizing shifts in inactivation recorded with I1327V and caused further hyperpolarizing shifts in activation curves. In view of these findings, patients with the I1327V mutation may achieve good seizure control with phenytoin in a manner similar to the patients reported in the study by Boerma et al.<sup>12</sup>

The mutation described herein has been observed in two patients to date. The first patient was a male child who experienced seizures immediately after birth and continued to experience refractory epilepsy until his death at the age of 1 year and 5 months.<sup>13</sup> It is unclear whether this patient was treated with phenytoin. The second patient was a male child who appeared to experience seizures in utero, perceived as “drumming” sensations during the later stages of pregnancy.<sup>19</sup> Although several AEDs were unsuccessful at providing seizure control in this patient, a high dose of phenytoin (18–20 mg/L) did provide temporary seizure control. Both patients had severe, early onset movement disorders. Our study demonstrates that these patients had a gain-of-function mutation of *SCN8A*, which likely accounted for their epileptic encephalopathy. The effectiveness of phenytoin at inhibiting the mutant channel currents provides additional evidence that phenytoin may be a useful treatment for *SCN8A* encephalopathy.

## ACKNOWLEDGMENTS

We are grateful to Drs. Sulayman Dib-Hajj and Stephen G. Waxman for providing the Na<sub>v</sub>1.6 cDNA. This work was supported by National Institutes of Health/National Institute for Neurological Disorders and Stroke grants (NINDS) R01NS075157 (MKP) and RO1NS34509 (MHM). JLW is a recipient of a postdoctoral fellowship from the Dravet Syndrome Foundation.

## DISCLOSURE

None of the authors has any conflict of interest to disclose. We confirm that we have read the Journal's position on issues involved in ethical publication and affirm that this report is consistent with those guidelines.



## REFERENCES

1. Cooper DC, Chung S, Spruston N. Output-mode transitions are controlled by prolonged inactivation of sodium channels in pyramidal neurons of subiculum. *PLoS Biol* 2005;3:e175.
2. Vreugdenhil M, Hoogland G, van Veelen CW, et al. Persistent sodium current in subicular neurons isolated from patients with temporal lobe epilepsy. *Eur J Neurosci* 2004;19:2769–2778.
3. Wagnon JL, Meisler MH. Recurrent and non-recurrent mutations of SCN8A in epileptic encephalopathy. *Front Neurol* 2015;6:104.
4. Blumenfeld H, Lampert A, Klein JP, et al. Role of hippocampal sodium channel Nav1.6 in kindling epileptogenesis. *Epilepsia* 2009;50:44–55.
5. Hargus NJ, Merrick EC, Nigam A, et al. Temporal lobe epilepsy induces intrinsic alterations in Na channel gating in layer II medial entorhinal cortex neurons. *Neurobiol Dis* 2011;41:361–376.
6. Hu W, Tian C, Li T, et al. Distinct contributions of Na(v)1.6 and Na(v)1.2 in action potential initiation and backpropagation. *Nat Neurosci* 2009;12:996–1002.
7. Boiko T, Van Wart A, Caldwell JH, et al. Functional specialization of the axon initial segment by isoform-specific sodium channel targeting. *J Neurosci* 2003;23:2306–2313.
8. Veeramah KR, O'Brien JE, Meisler MH, et al. De novo pathogenic SCN8A mutation identified by whole-genome sequencing of a family quartet affected by infantile epileptic encephalopathy and SUDEP. *Am J Hum Genet* 2012;90:502–510.
9. Blanchard MG, Willemsen MH, Walker JB, et al. De novo gain-of-function and loss-of-function mutations of SCN8A in patients with intellectual disabilities and epilepsy. *J Med Genet* 2015;52:330–337.
10. Estacion M, O'Brien JE, Conravey A, et al. A novel de novo mutation of SCN8A (Nav1.6) with enhanced channel activation in a child with epileptic encephalopathy. *Neurobiol Dis* 2014;69:117–123.
11. Wagnon JL, Korn MJ, Parent R, et al. Convulsive seizures and SUDEP in a mouse model of SCN8A epileptic encephalopathy. *Hum Mol Genet* 2015;24:506–515.
12. Boerma RS, Braun KP, van de Broek MPH, et al. Remarkable phenytoin sensitivity in 4 children with SCN8A-related epilepsy: a molecular neuropharmacological approach. *Neurotherapeutics* 2016;13:192–197.
13. Vaher U, Nõukas M, Nikopensius T, et al. De novo SCN8A mutation identified by whole-exome sequencing in a boy with neonatal epileptic encephalopathy, multiple congenital anomalies, and movement disorders. *J Child Neurol* 2014;29:202–206.
14. Herzog RI, Cummins TR, Ghassemi F, et al. Distinct repriming and closed-state inactivation kinetics of Nav1.6 and Nav1.7 sodium channels in mouse spinal sensory neurons. *J Physiol* 2003;551:741–750.
15. Wagnon JL, Barker BS, Hounshell JA, et al. Pathogenic mechanism of recurrent mutations of SCN8A in epileptic encephalopathy. *Ann Clin Transl Neurol* 2015;3:114–23; doi: 10.1002/acn3.276.
16. Remy S, Urban BW, Elger CE, et al. Anticonvulsant pharmacology of voltage-gated Na<sup>+</sup> channels in hippocampal neurons of control and chronically epileptic rats. *Eur J Neurosci* 2003;17:2648–2658.
17. Kuo CC, Bean BP. Slow binding of phenytoin to inactivated sodium channels in rat hippocampal neurons. *Mol Pharmacol* 1994;46:716–725.
18. Rogawski MA, Loscher W. The neurobiology of antiepileptic drugs. *Nat Rev Neurosci* 2004;5:553–564.
19. Singh R, Jayapal S, Goyal S, et al. Early-onset movement disorder and epileptic encephalopathy due to de novo dominant SCN8A mutation. *Seizure* 2015;26:69–71.
20. Smith MR, Goldin AL. Interaction between the sodium channel inactivation linker and domain III S4-S5. *Biophys J* 1997;73:1885–1895.
21. Ellerkmann RK, Remy S, Chen J, et al. Molecular and functional changes in voltage-dependent Na<sup>+</sup> channels following pilocarpine-induced status epilepticus in rat dentate granule cells. *Neuroscience* 2003;119:323–333.
22. Ketelaars SO, Gorter JA, van Vliet EA, et al. Sodium currents in isolated rat CA1 pyramidal and dentate granule neurones in the post-status epilepticus model of epilepsy. *Neuroscience* 2001;105:109–120.
23. Twombly DA, Yoshii M, Narahashi T. Mechanisms of calcium channel block by phenytoin. *J Pharmacol Exp Ther* 1988;246:189–195.
24. Lenkowski PW, Batts TW, Smith MD, et al. A pharmacophore derived phenytoin analogue with increased affinity for slow inactivated sodium channels exhibits a desired anticonvulsant profile. *Neuropharmacology* 2007;52:1044–1054.
25. Macdonald RL, Kelly KM. Mechanisms of action of currently prescribed and newly developed antiepileptic drugs. *Epilepsia* 1994;35 (Suppl. 4):S41–S50.
26. Meisler MH, Helman G, Hammer MF, Fureman BE, Gaillard WD, Goldin AL, Hirose S, Ishii A, Kroner BL, Lossin C, Mefford HC, Parent JM, Patel M, Schreiber J, Stewart R, Whittemore V, Wilcox K, Wagnon JL, Pearl PL, Vanderver A, Scheffer IE (2016) SCN8A Encephalopathy: Research Progress and Prospects. *Epilepsia*, June 8 Epub ahead of print.
27. Hille B. Local anesthetics: hydrophilic and hydrophobic pathways for the drug-receptor reaction. *J Gen Physiol* 1977;69:497–515.